Supplementary Information

Velocity analysis

The lithology of the newly identified LCVS is as of yet untested by wells, however understanding its lithology is crucial to understanding its evolution. Given that SDRs are considered to be predominantly volcanic in nature, the lateral continuity of SDRs into the LCVS (Fig. 5) implies that this package should also consist dominantly of volcanics. In the absence of well data, seismic velocity analysis is applied as it provides the best means of testing this model. Whilst seismic velocities are non-unique, strong and abrupt velocity variations in the subsurface can be used to differentiate volcanics from sediments as a consequence of the significant elastic contrast (Ogilvie et al., 2001). Here we apply semblance analysis to estimate velocities.

Semblance analysis technique

A 75 km portion of the seismic profile containing SDRs and the LCVS was chosen for semblance analysis using available pre-stack seismic data (Fig 4). Stacking velocities were not smoothed to allow us to analyse along-strike variations in velocity whilst also predicting lithology. Semblance analysis was undertaken every 250 m along the 75 km profile, resulting in 299 locations of analysis. To boost signal to noise ratio the analysis was undertaken on supergathers derived from the summation of 5 adjacent Common Mid-Point (CMP) gathers centring on the point of interest. An example of one such supergather is included in Suppl. Fig. 1, which also demonstrates that the stacking-velocity (V_{stack}) values picked correspond to strong semblance maxima in the semblance panel (column 1, Supp. Fig. 1).

Derivation of stacking velocity

Through picking stacking velocities across the seismic profile (Fig. 4**)** V_{stack}-depth (TWTT) trends can be plotted and used to identify major lithological variations. Mechanical compaction is an additional influence on velocity, with different lithologies being characterised by different compaction-depth trends. As compaction is controlled mainly by the thickness of the overlying sediment/rock column, with the effect of water depth being negligible, depth is calculated as TWTT below the seabed (Supp. Fig. 1). To compare stacking velocities, and hence infer differences in lithology between the SDR belt and the LCVS, V_{stack}-TWTT plots for the regions of the seismic profile (Fig. 4b) containing these two sequences are presented.

3896 stacking velocities were picked from 124 CMPs located over the SDR belt (Supp. Fig. 1 for velocity plots and Fig 4b for profile). Two V_{stack}-TWTT trends are evident and are separated by an abrupt change in gradient of the trend between 2500-2600 ms TWTT. This inflection correlates with the depth in the profile (in TWTT) of 6At1. The trend above this point, therefore, corresponds to the post-rift stratigraphy, whilst the trend beneath it corresponds to a volcanic-clastic SDR sequence (Supp. Fig. 1a). The two trends show slight overlap due to variations in post-rift thickness and structural relief along 6At1.

The V_{stack}-TWTT plot for the 44 km wide region of SPOB12 containing the LCVS is shown in Supp. Fig. 1b (location shown in Fig. 4b). The graph contains 3892 stacking velocities picked from 175 supergathers. As with the SDR belt, this plot also shows two distinct V_{stack}-TWTT trends, with the inflection point being located between 2700-2800 ms TWTT below the

seabed. This inflection point correlates with the approximate TWTT location of 6At1. Therefore, as was also observed over the SDR belt, two V_{stack}-TWTT trends are evident, one in the post-rift and one in the pre-breakup succession. The LCVS is often located vertically beneath the landward-most extent of the SDRs (Fig. 4b). However, no major change in V_{stack}-TWTT occurs between the SDRs located in this area and the LCVS which underlies them (as is annotated in Supp. Fig. 1b). This indicates that the SDRs and LCVS have a similar bulk composition.

Across the study area, two separate trends in the V_{stack}-TWTT plots are evident: one in the post-rift and one in the pre-breakup succession (Supp. Fig. 1a, Supp. Fig. 1b), regardless of whether this is occupied by SDRs or the LCVS. Ordinary least squares regression analysis allows us to compare the different V_{stack}-TWTT trends across the area. The post-rift V_{stack}-TWTT trends in both the SW (Supp. Fig. 1a) and the NE (Supp. Fig. 1b) of the profile are similar, having near identical gradients and intercepts. The V_{stack}-TWTT trends in the SDRs (Supp. Fig. 1A) and the LCVS (Supp. Fig. 1b) are also comparable to one another: the gradients (0.63 and 0.69 respectively) are similar and, although the intercepts are different, this is largely due to variations in post-rift thickness so that the depth to the inflection is different.

Throughout the study area velocity increases with depth, this indicates that the increase in velocity is partially controlled by the depth of burial. However, the differences in the velocity-depth trends (i.e. the difference between velocity-depth in the post-rift and the pre-breakup succession) are considered to be the result of changes in bulk lithology. We conclude from these results that there are two bulk lithologies in the area: one in the post-rift,

and one beneath 6At1, regardless of whether this consists of SDRs or the LCVS.

Predicting lithology from interval velocities

From the V_{stack}-TWTT trends (Supp. Fig. 1), it is clear that: 1) the LCVS has a very similar bulk lithology to the SDRs; and 2) that the SDRs and LCVS have a different bulk lithology to the post-rift. However, each stacking velocity is an average of the velocity in the entire rock column vertically overlying that point, hence, it is difficult to predict lithology directly from stacking velocities. Therefore, stacking velocities have been converted to interval velocities using the Dix Equation (Supp. Fig. 2c**,** Dix, 1955). An interval velocity is an approximation of the average p-wave velocity within a given interval and can be used to predict lithologies. In the post-rift, intervals were defined by major stratigraphic boundaries identified in the seismic profiles. In the SDRs and LCVS, intervals were defined by continuous reflectors and unconformities.

Two representative supergathers are shown in Supp. Fig. 2, one over the SDRs (Supp. Fig. 2a) and one over the LCVS (Supp. Fig. 2b). Therefore, these supergathers correspond to one supergather from Supp. Fig. 1a and one from Supp. Fig. 1b respectively. For each gather we show the semblance panel (column 1), the supergather (column 2), the interval velocities (column 3), and the supergather location on a PSTM seismic section (column 4). The semblance panel is included to demonstrate the validity of the V_{stack} picks and also to show how variations in the V_{stack}-TWTT gradient result in different interval velocities. The supergather demonstrates that the picks in the semblance panel relate to primary reflections, while the PSTM seismic section

permits changes in V_{int} and V_{stack}-TWTT to be correlated with the seismic stratigraphy described in earlier sections.

In the supergather located within the SDR belt (Supp. Fig. 2a), post-rift velocities increase progressively with depth with V_{int} ranging from 2162-3280 m/s. 6At1 marks a velocity increase of c. 1500 m/s, which is far larger than the velocity increases within the overlying post-rift intervals (573 m/s and 545 m/s). Underlying 6At1, interval velocities in the SDRs increase progressively with depth, ranging from 4780 to 5730 m/s. This supergather indicates that 6At1 marks a boundary between two bulk lithologies, as is marked by a major velocity increase. This supports the interpretation made from the V_{stack}-TWTT data (Supp. Fig. 1a).

The supergather located over the LCVS (Supp. Fig. 2b) also shows a change in bulk lithology with depth, however, here this occurs in the lowermost post-rift (Supp. Fig. 2b) and not at 6At1. The post-rift succession overlying the LCVS has been divided into four intervals. The upper three have velocities that are similar to those in the post-rift described above, with V_{int} increasing with depth from 2217-3335 m/s (Supp. Fig. 2b). The lowermost post-rift interval is relatively thin (0.18 s TWTT) and is defined by a major velocity increase: V_{int} is 4947 m/s, requiring an increase of 1612 m/s. There is no unconformity at the top of this package, indicating that the velocity increase results from a change in bulk lithology. Beneath this high velocity package, V_{int} increases progressively with depth (Supp. Fig. 2b). The interval directly underlying 6At1 consists of SDRs and has a V_{int} of 5160 m/s. These SDRs are underlain by the LCVS where V_{int} increases with depth from 5160-6064 m/s. As was suggested by the V_{stack}-TWTT data, the velocities in the

LCVS are similar to those in the SDRs, which indicates that they have similar lithologies.

The interval velocities of the post-rift (typically from 2100-3500 m/s) are typical of a thick clastic succession, where the increase of velocity with depth is controlled principally by compaction. Lithological variations, such as varying sand content, are likely to result in the scatter observed in the V_{stack}-TWTT data.

The calculated interval velocities within the SDRs and LCVS fall within a range typical of flood basalt successions on magma-rich margins (Calvès et al., 2011; Eldholm and Grue, 1994). Whilst clastic sediments may be interbedded with these volcanics, as has been observed on the Norwegian Margin (Mutter et al., 1982), the velocities observed in the SDRs and LCVS indicates that they consist dominantly of volcanics. Velocities within the volcanic succession increase with depth, which is likely an effect of compaction and alteration (Eldholm and Grue, 1994).

In Supp. Fig. 2b we also observe a major velocity increase in the lowermost post-rift. Volcanics within the earliest post-rift have been identified elsewhere on the margin (Gerrard and Smith, 1982; Light et al., 1993), including possibly in this study (the volcanic mound in Fig. 3). Hence this velocity jump is also likely to be a result of volcanics emplaced during the earliest stages of the post-rift.

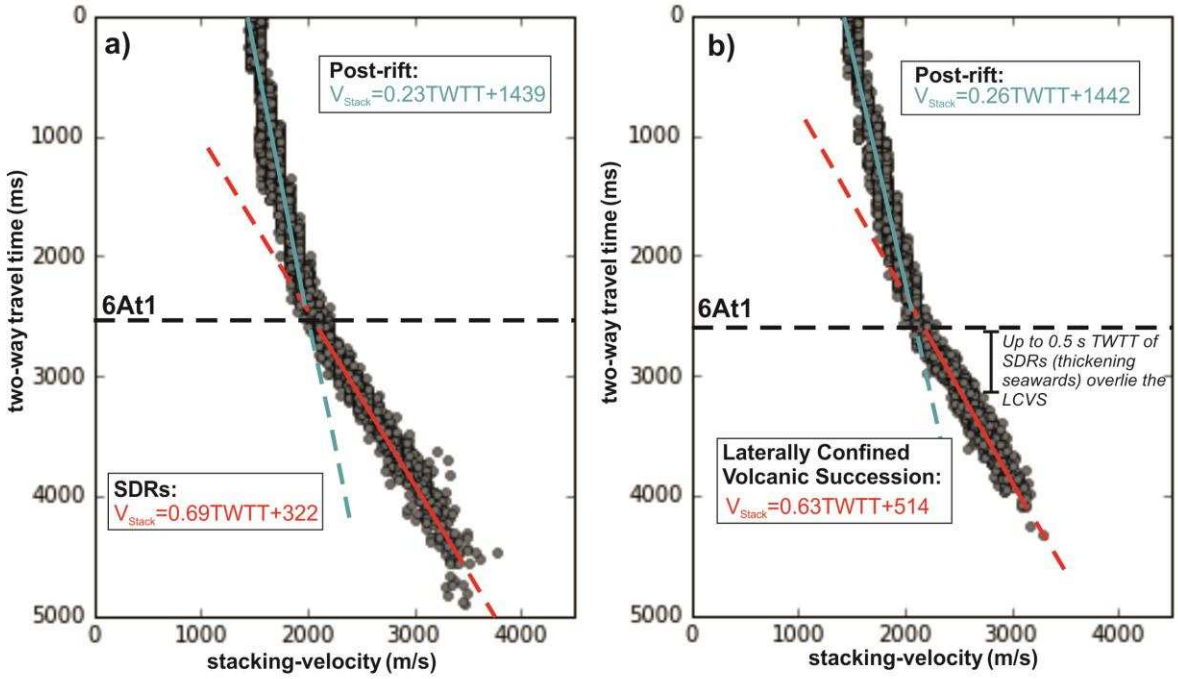

Supp. Fig. 1. a) Graph showing stacking velocity (V_{stack}) vs two-way travel time (TWTT) in the region of **Fig. 4b** overlying the SDRs. b) Graph showing stacking velocity vs two-way travel time in the region of **Fig. 4b** overlying the Laterally Confined Volcanic Succession. In both graphs the approximate TWTT of 6At1 is annotated, as are the V_{stack}-TWTT relationships for the different megasequences.

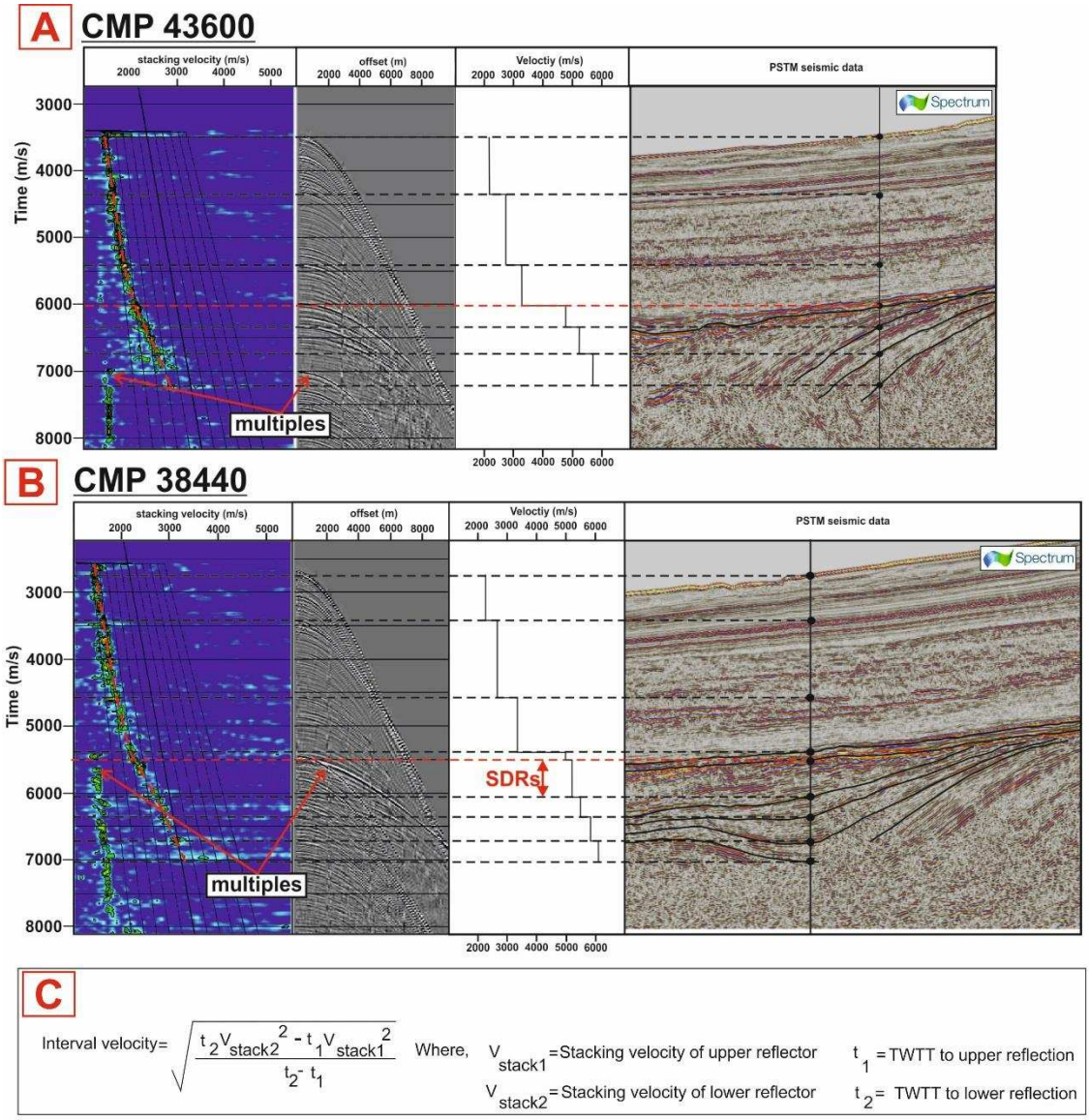

Supp. Fig. 2. Representative CMP gathers located over the SDRs (a) and the Laterally Confined Volcanic Succession (b). Both a) and b) consist of four columns: Column 1 shows the semblance panel with the V_{stack}-TWTT trend annotated (red dashed line). Column 2 shows the supergather, column 3 shows the interval velocities, and column 4 shows PSTM seismic data. Key horizons are correlated across all columns, these horizons bound the intervals in columns 3 and 4. c) shows the Dix equation, which is used for converting stacking velocities to interval velocities.

References:

Calvès, G., Schwab, A.M., Huuse, M., Clift, P.D., Gaina, C., Jolley, D., Tabrez, A.R., Inam, A., 2011. Seismic volcanostratigraphy of the western Indian rifted margin: The pre-Deccan igneous province. J. Geophys. Res. 116, B01101. https://doi.org/10.1029/2010JB000862

Dix, C.H., 1955. Seismic Velocities From Surface Measurements. Geophysics 20, 68–86. https://doi.org/10.1190/1.1438126

Eldholm, O., Grue, K., 1994. North Atlantic volcanic margins : Dimensions and production rates a volume of flood basalts a mean eruption rate of the basalts were emplaced within volume in a mean crustal accretion rate. J. Geophys. Res. 99, 2955–2968.

Gerrard, I., Smith, G., 1982. Post-Paleozoic succession and structure of the southwestern African continental margin. Stud. Cont. margin Geol. AAPG Mem.

Light, M.P.., Maslanyj, M.P., Greenwood, R.J., Banks, N.L., 1993. Seismic sequence stratigraphy and tectonics offshore Namibia. Geol. Soc. London Spec. Publ. 71, 163–191.

Mutter, J., Talwani, M., Stoffa, P., 1982. Origin of seaward-dipping reflectors in oceanic crust off the Norwegian margin by “subaerial sea-floor spreading.” Geology 10, 353–357.

Ogilvie, J.S., Crompton, R., Hardy, N.M., 2001. Characterization of volcanic units using detailed velocity analysis in the Atlantic Margin, West of Shetlands, United Kingdom. Lead. Edge 20, 34–50. https://doi.org/10.1190/1.1438874